Materials Science & Engineering A 654 (2016) 418–425

Contents lists available at ScienceDirect

Materials Science & Engineering A

journal homepage: www.elsevier.com/locate/msea

Characterization of fatigue properties of powder metallurgy titanium alloy

Yuankui Cao [a], Fanpei Zeng [b], Bin Liu [a,b,*], Yong Liu [a,**], Jinzhong Lu [b], Ziyang Gan [a], Huiping Tang [c]

[a] State Key Lab of Powder Metallurgy, Central South University, Changsha 410083, PR China
[b] Fujian Longxi Bearing (Group) Corp., LTD, Zhangzhou 363000, PR China
[c] State Key Lab of Porous Metal Materials, Northwest Institute for No-ferrous Metal Research, Xian 710016, PR China

ARTICLE INFO

Article history:
Received 7 September 2015
Received in revised form
23 November 2015
Accepted 17 December 2015
Available online 19 December 2015

Keywords:
Titanium alloys
Powder metallurgy
Hot deformation
Fatigue
Microtexture
EBSD

ABSTRACT

The fatigue characteristics of powder metallurgy (P/M) Ti6Al4V (wt%) alloys prepared by powder sintering and hot rolling were studied under tension–tension loading conditions at $R=0.1$ and 25 Hz in air, where $R=\sigma_{min}/\sigma_{max}$ (σ_{min} and σ_{max} are the applied minimum and maximum stresses, respectively). The results show that for the as-sintered Ti6Al4V alloy the fatigue limit is about 325 MPa, and the fatigue cracks initiate from the residual pores open to the surface of the gauge area and propagate along the α/β interfaces. Hot rolling markedly enhances the fatigue properties, and the fatigue limit increases to about 430 MPa. The reducing of porosity and refining of grain size through hot rolling are the dominant mechanisms for the improvement of fatigue properties. In addition, the microstructure of α/β interfaces//RD and the texture of <0001>α//RD formed during hot rolling act as barriers for the fatigue crack propagation, which partly attributes to the improvement of the fatigue properties.

1. Introduction

Titanium alloy weighs approximately 50% less than steel or corrosion resistant alloy, which makes titanium alloy an excellent structural material in both aerospace and automotive industries [1–4]. The wider application of titanium alloy products is limited by the high cost of the raw material and its treatment, which is why manufacturing methods that provide reduction of the final cost are needed [5]. Powder Metallurgy (P/M) approach is a viable and promising route for cost-effective fabrication of titanium components due to the usage of low-cost raw materials, high workability and near net shaping. For some high-end parts, the cost savings can be as high as 50–70% [6]. Along with a reduction of the cost of products manufactured using P/M method, a decrease in their mechanical characteristics (especially the fatigue properties) occurs compared with the products made of cast and especially hot deformed alloys.

The fatigue resistances of the titanium alloys are most sensitive to the microstructures. For titanium materials with shrinkage defects or residual pores, the fatigue cracks were found to initiate from the clusters of pores either at the surface or at the near subsurface [7]. The quantity and size of pores decided the fatigue crack initiation period. At a porosity of 1–2%, the fatigue resistance decreased by 10–30%. However, the static mechanical characteristics were not markedly influenced by the residual pores [1]. The fatigue properties are also closely related to the grain/phase microstructure. Goldenet al. [8] and Bridier et al. [9] found that decreasing the primary α grain size can shorten the slip length and improve the fatigue crack initiation resistance, thus improving the fatigue resistance. During the crack propagation, Guo et al. [10] and Ghonem et al. [11] found that the path of the crack spread along the α/β lamella interfaces in lamellar titanium alloys, therefore, adjusting the orientation of α/β interfaces may have positive effects on improving fatigue properties.

To lower the level of residual porosity and improve the mechanical characteristics of P/M titanium alloys, a complicated and costly hot isostatic pressing (HIP) technology is often applied, but even the use of this technology does not always lead to a complete densitification, but causes obvious coarsening of the microstructure. Plastic deformation is one of the most effective ways to densitify P/M materials, and is often used in P/M titanium alloys, ferrite alloys and copper alloys. Plastic deformation can also refine the sintered microstructure, rearrange the α/β lamella interfaces, and explore macrotexture in titanium alloys [12–14]. Therefore, plastic deformation may have a positive effect on the fatigue

* Corresponding author at: State Key Lab of Powder Metallurgy, Central South University, Changsha 410083, PR China.
** Corresponding author.
E-mail addresses: binliu@csu.edu.cn (B. Liu), yonliu@csu.edu.cn (Y. Liu).

http://dx.doi.org/10.1016/j.msea.2015.12.058
0921-5093/

properties. Up to now, the available data for fatigue properties of P/M titanium alloys is limited. Specifically, the fatigue limit, which serves as a criterion for the applicability of structural materials in many cases, remains unexplored.

The objective of the present work is to determine the fatigue resistances of the Ti6Al4V alloys obtained through P/M method, clarify the fatigue deformation mechanism and figure out the effects of plastic deformation on fatigue resistance characteristics.

2. Materials and experimental procedures

The hydride-dehydride Ti powders and pre-alloyed Al–V powders were used as raw materials to fabricate the P/M Ti6Al4V alloys. The average particle sizes of Ti and Al–V powders are about 23 µm and 40 µm, respectively. The chemical compositions of the raw powders are shown in Table 1. The raw powders were blended with a high efficient blender for 8 h under argon atmosphere, and then were compressed via Cold Isostatic Pressing (CIP) with a pressure of 180 MPa. The mixed powders were easy to stack densely during CIP due to the uneven particle size, and subsequently gained a green density of 3.67 g/cm^3. The green compacts were sintered at 1250 °C with a holding time of 2 h in a vacuum of 1×10^{-3} Pa followed by furnace cooling. The dimension of the sintered bars was 450 mm in length and 43 mm in diameter. After sintering, the as-sintered bars were hot-rolled at 890 °C to different sizes.

Three kinds of samples were used to study the fatigue properties. Sample A was cut from the as-sintered bars, and sample B and C were cut from the hot-rolled bars. The characteristics of the three samples were listed in Table 2. Fatigue specimens with a round shape were machined from the hot-rolled bars along the rolling direction (RD) because the round edged sample has a higher fatigue endurance limit and stability than the sharp edged sample [7]. The dimension of the fatigue specimen are shown in Fig. 1. The fatigue testing was followed the ASTM Standard E466-07. Emery papers of #2000 were used to ground and polish the surface of the specimens. Fatigue tests were carried out on a INSTRON 8802 test machine in air, with a cyclic frequency of 25 Hz and a stress ratio of R=0.1. Maximum stresses (σ_{m}) ranging from 325 to 800 MPa with a loading form of sinusoidal wave were applied to figure out the fatigue limit. The fatigue endurance limit or the "runout" of the fatigue tests was defined as 10^7 cycles. Scanning electronic microscopy (SEM) and Electron Back-Scattered Diffraction (EBSD) were performed to study the microstructures and the fatigue fractographs of the P/M Ti6Al4V alloys. The density of the P/M Ti6Al4Vsamples was measured by the Archimedes method.

Table 1
Interstitial element contents of the titanium powders and the pre-alloyed Al–V powders.

Element (ppm)	Ti powders	Al–V powders
O 3500 4700 C 350 120 N 76 67 H 10 4		

Table 2
States and density of the P/M Ti6Al4Vsmaples.

Samples	Degrees of deformation (%)	Density (g/cm^3)	Relative density (%)	Standard deviation of relative density (%)
Sample A	0	4.35	96.5	0.3
Sample B	56	4.40	99.2	0.27
Sample C	104	4.41	99.7	0.17

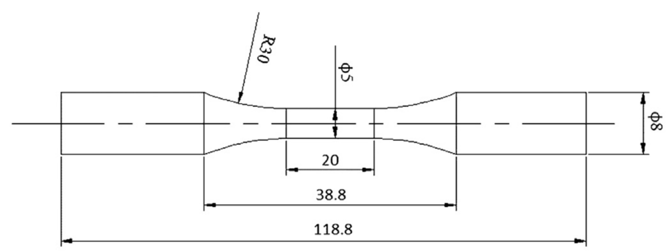

Fig. 1. Dimension of the P/M Ti6Al4V fatigue specimen (mm).

3. Results

3.1. Microstructure and tensile properties of the P/M Ti6Al4V alloys

Fig. 2 shows the microstructures of the as-sintered and hot-rolled P/M Ti6Al4V alloys. The as-sintered sample (Fig. 2a and b) shows a lamellar microstructure with the colony size of about 50 µm. Some residual pores with round shape distribute on the matrix, and the porosity is about 3.5%. After hot rolling to a deformation of 56% (Fig. 2c and d), the residual pores are effectively eliminated, and the porosity decreases to about 0.8%. The lamellar microstructure is destroyed, and part of the β phase elongates along the RD. With the deformation increase to 104% (Fig. 2e and f), the grain structure becomes finer and the porosity further decreases to about 0.3%, the microstructure forms an obvious fibrous microstructure along the RD. Fig.3 shows the ultimate tensile strength (UTS) and elongation (El) of the P/M Ti6Al4V samples. The mechanical properties tests were carried out along RD. In the as-sintered state, the UTS and El are 1020 MPa and 5%, respectively. After a deformation of 56%, the UTS and El increase to 1100 MPa and 11%, respectively. With the deformation further increases to 104%, the UTS and El further increase to 1205 MPa and 12%, respectively.

3.2. Fatigue behavior of the P/M Ti6Al4V alloys

Fig. 4 shows the S–N curves of the P/M Ti6Al4V alloys. It is indicated that the fatigue endurance increases with maximum cyclic stress (σ_m, Mpa) decreasing, and turns stable when the cyclic number (N_f) reaches around 10^7. The fatigue limit (σ_l) for the as-sintered sample is about 325 MPa, while the values for the hot-rolled sample B and C are 400 MPa and 430 MPa, respectively. The fractographs of the hot-rolled sample (sample C) are shown in Fig. 5. Three typical fatigue stages can be found on the fracture surface (Fig. 5a): the crack initiation site, the crack propagation region, and the fast fracture region. Fig. 5b shows the crack initiation site. The river patters indicate that the fatigue crack initiates from a surface pore. It is found that the crack initiations of all the specimens are located on the surface of the samples. After initiating, cracks start to propagate towards the center of the specimen. The crack propagation region shows a flat and striated type fracture surface (Fig. 5c), which is mainly due to the repeated resharpening and blunting process during cyclic loading. With the fatigue crack propagating, the area of effective stress-bearing surface reduces, which leads to an increase in the true cyclic stress. Once the true cyclic stress achieves a critical state that is sufficient to break the specimen, a momentary break takes place immediately, and a dimple structure on the fast fracture region is produced, as shown in Fig. 5d. The fast fracture region is much rougher than the crack propagation region and occupies most of